

Interpretation of $\Omega(2012)$ as a $\Xi(1530)K$ molecular state

Xiang Yu¹, Jin-Peng Zhang¹, Xu-Liang Chen¹, Ding-Kun Lian², Qi-Nan Wang³, and Wei Chen^{1,4*}

¹*School of Physics, Sun Yat-sen University, Guangzhou 510275, China*

²*School of Physics, Southeast University, Nanjing 210094, China*

³*College of Physical Science and Technology, Bohai University, Jinzhou 121013, China*

⁴*Southern Center for Nuclear-Science Theory (SCNT), Institute of Modern Physics, Chinese Academy of Sciences, Huizhou 516000, Guangdong Province, China*

We investigate the mass and strong decay properties of the $\Omega(2012)$ resonance using QCD sum rules, assuming it to be an S-wave $\Xi(1530)K$ molecular pentaquark state with $IJ^P = 0\frac{3}{2}^-$. A unified interpolating current is constructed, and the two-point and three-point correlation functions are calculated up to dimension-10 condensates in the OPE series. The negative-parity contribution is isolated by employing parity-projected sum rules. The two-body strong decays to $\Xi^0 K^-$ and $\Xi^- K^0$ are studied via their three-point correlation functions. Our analysis yields a mass of 2.00 ± 0.15 GeV and a total two-body decay width of $\Gamma = 3.97^{+8.31}_{-1.92}$ MeV for the $\Xi(1530)K$ molecular state. The ratios of branching fractions are obtained as $\mathcal{R}_{\Xi^0 K^-}^{\Xi^- K^0} = 0.85$ and $\mathcal{R}_{\Xi K}^{\Xi \pi K} = 0.61$. These results are compatible well with the experimental data for the $\Omega(2012)$ and support its interpretation as a $\Xi(1530)K$ molecular pentaquark state.

Keywords: Molecular pentaquark state, QCD sum rules, Correlation functions, Branching fraction

I. INTRODUCTION

Quantum chromodynamics (QCD) is the fundamental theory of the strong interaction. While conventional hadrons are well described as quark-antiquark mesons and three-quark baryons in the quark model [1, 2], QCD also permits the existence of exotic hadron states such as multi-quark states, hybrid mesons, glueballs and so on. Detailed discussions can be found in recent comprehensive reviews [3–17].

In 2018, the Belle Collaboration first observed a narrow structure, denoted $\Omega(2012)$, in the $\Xi^0 K^-$ and $\Xi^- K_S^0$ invariant mass spectra, providing the first experimental evidence for this excited Ω baryon [18]. Prior to this discovery, the mass spectrum of the Ω family had been extensively studied using various theoretical approaches [19–37], many of which predicted a pair of negative-parity excited Ω^- states with $J^P = \frac{1}{2}^-$ and $J^P = \frac{3}{2}^-$ in the mass region near 2 GeV. The existence of the $\Omega(2012)$ was subsequently reinforced by Belle through its observation in weak decays of the Ω_c baryon, offering an independent production channel and further consolidating its resonance nature [38]. More recently, the ALICE Collaboration reported the discovery of $\Omega(2012)$ with a significance of 15σ in pp collisions at the LHC [39], while the BESIII Collaboration presented evidence for a new production mechanism of this state via the process $e^+e^- \rightarrow \Omega(2012)\bar{\Omega}^+ + c.c.$ with a significance of 3.5σ [40]. In PDG [41], the mass and total decay width of $\Omega(2012)$ are collected to be $m = 2012.4 \pm 0.9$ MeV and $\Gamma = 6.4^{+3.0}_{-2.6}$ MeV, and the branching fraction ratio $\mathcal{R}_{\Xi^0 K^-}^{\Xi^- K^0} = 0.83 \pm 0.21$.

The discovery of this multistrange resonance has stimulated considerable theoretical interest, which focused on two broad interpretive frameworks. One framework regards $\Omega(2012)$ as a conventional excited baryon. In particular, based on its relatively narrow width, it has been argued that the most likely spin-parity assignment is $J^P = \frac{3}{2}^-$ [42–54]. The alternative picture describes $\Omega(2012)$ as a meson–baryon molecular state dominated by the Ξ^*K configuration with $J^P = \frac{3}{2}^-$ [55–68]. Within this molecular scenario, the generation of a $J^P = \frac{1}{2}^-$ state is generally disfavored. This interpretation is motivated by the mass of $\Omega(2012)$ lying close to the $\Xi(1530)K$ threshold. Notably, both scenarios are capable of reproducing key experimental observables, such as the mass, narrow width, and production in Ω_c decays, suggesting that the physical $\Omega(2012)$ state may involve a nontrivial interplay between compact three-quark and meson–baryon components [53, 69]. A comprehensive overview of the experimental and theoretical status of $\Omega(2012)$ can be found in the recent reviews [66, 70].

A crucial distinction between these competing interpretations arises from their predictions for decay patterns, particularly the three-body decay channels. Conventional three-quark models generally favor dominant two-body $K\Xi$ decays, with the three-body $K\pi\Xi$ mode being strongly suppressed. In contrast, molecular scenarios naturally allow for sizable contributions from the $K\pi\Xi$ channel due to strong meson–baryon couplings. Experimentally, early analyzes reported no evidence for such three-body decays [71]. However, subsequent measurements by Belle Collaboration revisited this issue and reported the experimental value $\mathcal{R}_{\Xi K}^{\Xi \pi K} = 0.99 \pm 0.26 \pm 0.06$ [72]. More recently, the ALICE Collaboration reported the branching fraction for the two-body decay channel as $\mathcal{B}[\Omega^* \rightarrow \Xi K] = 0.62^{+0.27}_{-0.17}$ in 2025 [39]. Assuming that all $\Omega(2012)$ decays proceed exclusively via

*Electronic address: chenwei29@mail.sysu.edu.cn

either $\Omega(2012) \rightarrow \Xi K$ or $\Omega(2012) \rightarrow \Xi\pi K$, the ALICE result is consistent with the Belle measurement within the uncertainties.

In this paper, we employ QCD sum rules to carry out a systematic investigation of the mass and the two-body decay width of $\Omega(2012)$, treating it as an S-wave $\Xi(1530)K$ molecular pentaquark state. Our calculations for both the mass and the two-body decay properties of the $\Omega(2012)$ are consistent with the available experimental results, supporting its interpretation as a $\Xi(1530)K$ molecular pentaquark with $J^P = \frac{3}{2}^-$. Nevertheless, a definitive conclusion requires a further analysis of its three-body decay channels, which we leave for future work.

This paper is organized as follows. In Sec. II, we introduce the interpolating currents and outline the QCD sum rules analysis. Sec. III presents the numerical results of hadron mass and two-body strong decays. Finally, concluding remarks are provided in Sec. IV.

II. TWO-POINT AND THREE-POINT QCD SUM RULES

A. The $\Xi(1530)K$ molecular interpolating current with $J^P = 3/2^-$

In this subsection, we construct an interpolating current that describes a meson–baryon molecular state with $J^P = \frac{3}{2}^-$. The interpolating current for the K meson is given by

$$J_K(x) = \bar{q}^d(x) i\gamma_5 s^d(x), \quad (1)$$

while the current for the $\Xi(1530)$ baryon with $J^P = \frac{3}{2}^+$ reads

$$J_{\Xi^*}(x) = \sqrt{\frac{1}{3}} [2s^{aT}(x) \mathcal{C} \gamma_\mu q^b(x) s^c(x) + s^{aT}(x) \mathcal{C} \gamma_\mu s^b(x) q^c(x)], \quad (2)$$

in which a, b, c, d are color indices, and $\mathcal{C} = i\gamma_2\gamma_0$, s and q are the strange and light (u/d) quark fields respectively. The current J_{Ξ^*} has been widely adopted in QCD sum rules of decuplet baryons [73]. One shall find the currents J_{K^-} and $J_{\Xi^{*0}}$ for $q = u$, while the currents J_{K^0} and $J_{\Xi^{*-}}$ for $q = d$ in Eqs. (1)-(2). Then we can construct an S-wave $\Xi^* \bar{K}$ molecular pentaquark current with $J^P = \frac{3}{2}^-$ as

$$\eta_\mu = \sqrt{\frac{1}{3}} \epsilon^{abc} [\bar{q}^d(x) i\gamma_5 s^d(x)] [2(s^{aT}(x) \mathcal{C} \gamma_\mu q^b(x)) s^c(x) + (s^{aT}(x) \mathcal{C} \gamma_\mu s^b(x)) q^c(x)]. \quad (3)$$

It is worth emphasizing that alternative pentaquark currents can also be constructed with the same quantum

numbers but different Dirac structures, such as

$$\sqrt{\frac{1}{3}} \epsilon^{abc} [\bar{q}^d(x) i\gamma_5 s^d(x)] [2(s^{aT}(x) \mathcal{C} \gamma_\mu q^b(x)) \sigma_{\mu\nu} s^c(x) + (s^{aT}(x) \mathcal{C} \gamma_\mu s^b(x)) \sigma_{\mu\nu} q^c(x)] \quad (4)$$

or

$$\sqrt{\frac{1}{3}} \epsilon^{abc} [\bar{q}^d(x) i\gamma_5 s^d(x)] [2(s^{aT}(x) \mathcal{C} \sigma_{\mu\nu} q^b(x)) \gamma_\mu s^c(x) + (s^{aT}(x) \mathcal{C} \sigma_{\mu\nu} s^b(x)) \gamma_\mu q^c(x)]. \quad (5)$$

A Fierz rearrangement, however, reveals that these currents are not independent but are equivalent to one another [74]. It follows that, within this construction, Eq. (3) represents the unique interpolating current for the $J^P = 3/2^-$ $\Xi(1530)K$ molecular state.

Considering the isoscalar nature of $\Omega(2012)$, one can finally achieve the interpolating current coupling to this state as

$$J_\mu(x) = \frac{1}{\sqrt{2}} (J_{\Xi^{*0}} \cdot J_{K^-} - J_{\Xi^{*-}} \cdot J_{K^0}). \quad (6)$$

In the following analyses, we shall use this current to study the hadron mass and the strong decay properties of $\Omega(2012)$.

B. Two-point correlation function

The molecular interpolating current J_μ in Eq. (6) can couple to both the negative-parity and positive-parity states through different coupling relations

$$\langle 0 | J_\mu | \Omega^*; 3/2^- \rangle = f_- u_\mu(p), \quad (7)$$

$$\langle 0 | J_\mu | \Omega^{*'}; 3/2^+ \rangle = f_+ \gamma_5 u_\mu(p), \quad (8)$$

where f_\pm are coupling constants and $u_\mu(p)$ is the Rarita-Schwinger vector-spinor. Thus, the two-point correlation function induced by such a current contains both information. It can be written as

$$\begin{aligned} \Pi_{\mu\nu}(p^2) &\equiv i \int d^d x e^{ip \cdot x} \langle 0 | T [J_\mu(x) \bar{J}_\nu(0)] | 0 \rangle \\ &= -g_{\mu\nu} \Pi_{3/2}(p^2) + \dots, \end{aligned} \quad (9)$$

where $\Pi_{3/2}(p^2)$ is the invariant function corresponding to the hadron states with $J^P = \frac{3}{2}^\pm$ [75, 76].

On the phenomenological side, by inserting a complete set of intermediate states, the correlation function can be expressed as

$$\begin{aligned} \Pi_{\mu\nu}^{\text{phe}}(p^2) &= -g_{\mu\nu} \left[(f_-)^2 \frac{\not{p} + m_-}{m_-^2 - p^2} + (f_+)^2 \frac{\not{p} - m_+}{m_+^2 - p^2} \right] + \dots \\ &= -g_{\mu\nu} \left[\Pi_{\not{p}}^{\text{phe}}(p^2) \not{p} + \Pi_I^{\text{phe}}(p^2) \right] + \dots \end{aligned} \quad (10)$$

The invariant function $\Pi(p^2)$ can be described by the dispersion relation

$$\Pi(p^2) = (p^2)^n \int_0^\infty \frac{\rho(s)}{s^n(s-p^2)} ds + \sum_{k=0}^{n-1} a_k (p^2)^k, \quad (11)$$

where a_k is the subtraction constant and $\rho(s) = \frac{1}{\pi} \text{Im} \Pi(s)$ is defined as the spectral function. According to Eqs. (10)-(11), one finds the following two spectral functions

$$\begin{aligned} \rho_{\not{p}}^{\text{phen}}(s) &= f_-^2 \delta(s - m_-^2) + f_+^2 \delta(s - m_+^2), \\ \rho_I^{\text{phen}}(s) &= f_-^2 m_- \delta(s - m_-^2) - f_+^2 m_+ \delta(s - m_+^2), \end{aligned} \quad (12)$$

from which we can separate the spectral densities for negative- and positive-parity states as

$$\rho_{\mp}^{\text{phe}} = \sqrt{s} \rho_{\not{p}}^{\text{phe}}(s) \pm \rho_I^{\text{phe}}(s). \quad (13)$$

At the quark-gluon level, the correlation function is computed using the operator product expansion (OPE), expressed in terms of quark masses and various QCD parameters. We adopt the d -dimensional coordinate-space expression for the light quark propagator [77]

$$\begin{aligned} S^{ij}(x) &= \frac{i\Gamma(\frac{d}{2}) \not{x}}{2\pi^{d/2}(-x^2)^{d/2}} \delta^{ij} + \frac{m\Gamma(\frac{d}{2}-1)}{4\pi^{d/2}(-x^2)^{d/2-1}} \delta^{ij} - \frac{\delta^{ij}}{12} \langle \bar{\psi}\psi \rangle + \frac{im\delta^{ij}}{12d} \langle \bar{\psi}\psi \rangle \not{x} - \frac{\delta^{ij}}{48d} \langle g\bar{\psi}\sigma G\psi \rangle x^2 \\ &\quad - \frac{i\delta^{ij}x^2 \not{x}}{2^4 3^4 (d+2)} g^2 \langle \bar{\psi}\psi \rangle^2 + \frac{i\delta^{ij}mx^2 \not{x}}{2^4 3d(d+2)} \langle g\bar{\psi}\sigma G\psi \rangle - \frac{\delta^{ij}x^4 \langle \bar{\psi}\psi \rangle \langle g^2 G^2 \rangle}{2^6 3^2 d(d+2)} - \frac{\delta^{ij}x^4}{2^4 3^4 d(d+2)} g^2 m \langle \bar{\psi}\psi \rangle^2 \\ &\quad - \frac{i\delta^{ij}\Gamma(\frac{d}{2}-1) \not{x} \langle g^3 f G^3 \rangle}{2^8 3^3 d(d+2) \pi^{d/2} (-x^2)^{d/2-3}} + \frac{\Gamma(\frac{d}{2}-1) \gamma^\mu \not{x} \gamma^\nu}{16\pi^{d/2} (-x^2)^{d/2-1}} g G_{\mu\nu}^a T_{ij}^a \\ &\quad + \left[\frac{\Gamma(\frac{d}{2}-2) (\gamma^{\mu\rho\nu} + \gamma^{\rho\mu\nu} - 4g^{\mu\rho}\gamma^\nu)}{96\pi^{d/2} (-x^2)^{d/2-2}} + \frac{\Gamma(\frac{d}{2}-1) (x^\mu \gamma^\rho \not{x} \gamma^\nu + x^\rho \gamma^\mu \not{x} \gamma^\nu)}{48\pi^{d/2} (-x^2)^{d/2-1}} \right] g G_{\mu\nu;\rho}^a T_{ij}^a \\ &\quad + \left(\frac{-\Gamma(\frac{d}{2}-2) (2g^{\{\mu\rho}x^\sigma\} + g^{\{\mu\rho}\gamma^\sigma\} \not{x})}{2^8 \times 3\pi^{d/2} (-x^2)^{d/2-2}} + \frac{\Gamma(\frac{d}{2}-1) x^{\{\mu}x^\rho\gamma^\sigma\} \not{x}}{192\pi^{d/2} (-x^2)^{d/2-1}} \right) \gamma_\nu g G_{\mu\nu;\rho\sigma}^a T_{ij}^a \\ &\quad + g^2 G_{\mu\nu}^a G_{\rho\sigma}^b (T^a T^b)_{ij} \left[\frac{-i\Gamma(\frac{d}{2}-1) x^\nu x^\sigma \gamma^\mu \not{x} \gamma^\rho}{96\pi^{d/2} (-x^2)^{d/2-1}} + \frac{-i\Gamma(\frac{d}{2}-2) g^{\nu\sigma} \gamma^\mu \not{x} \gamma^\rho}{192\pi^{d/2} (-x^2)^{d/2-2}} \right. \\ &\quad \left. + \frac{i\Gamma(\frac{d}{2}-2)}{2^8 \times 3\pi^{d/2} (-x^2)^{d/2-2}} (-6g^{\nu\sigma} \not{x} \gamma^{\mu\rho} - 4x^\sigma \gamma^{\mu\nu\rho} + 6x^\mu \gamma^{\nu\rho\sigma} - 4x^\nu \gamma^{\mu\sigma\rho} + 3\gamma^\mu \not{x} \gamma^{\nu\rho\sigma}) \right], \end{aligned} \quad (14)$$

where m is the light quark mass, $i, j = 1, 2, 3$ are color indices, and $T^a (a = 1, \dots, 8)$ is the Gell-Mann matrix. The related abbreviations are defined as

$$\begin{aligned} \gamma^{\mu\nu\rho} &:= \gamma^\mu \gamma^\nu \gamma^\rho, \quad g^{\{\mu\rho}x^\sigma\} := g^{\mu\rho}x^\sigma + g^{\mu\sigma}x^\rho + g^{\rho\sigma}x^\mu, \\ g^{\{\mu\rho}\gamma^\sigma\} &:= g^{\mu\rho}\gamma^\sigma + g^{\mu\sigma}\gamma^\rho + g^{\rho\sigma}\gamma^\mu, \\ x^{\{\mu}x^\rho\gamma^\sigma\} &:= x^\mu x^\rho \gamma^\sigma + x^\mu x^\sigma \gamma^\rho + x^\rho x^\sigma \gamma^\mu, \\ G_{\mu\nu;\rho}^a &:= \tilde{D}_\rho^{ab} G_{\mu\nu}^b, \quad G_{\mu\nu;\rho\sigma}^a := \tilde{D}_\sigma^{ab} \tilde{D}_\rho^{bc} G_{\mu\nu}^c, \end{aligned} \quad (15)$$

in which $G_{\mu\nu}$ is the gluon field strength, $\tilde{D}_\mu^{ab} = \delta^{ab}\partial_\mu - g f^{abc} A_\mu^c$ is the covariant derivative operator in the adjoint representation, and A_μ^c is the external gauge field. This propagators can guaranteed the infrared (IR) safety for the calculations involving the tri-gluon condensate $\langle g^3 f G^3 \rangle$ [77].

We preserve the calculations of spectral functions $\rho_{\not{p}}^{\text{OPE}}(s)$ and $\rho_I^{\text{OPE}}(s)$ up to dimension 10, and the corresponding Feynman diagrams are shown in Fig. 1. The

results of $\rho_{\not{p}}^{\text{OPE}}(s)$ and $\rho_I^{\text{OPE}}(s)$ are too lengthy to present here, so we list them in Appendix A.

Due to the principle of quark-hadron duality, the correlation function computed at the quark-gluon level is expected to be equivalent to the one at the hadron level. Then the Borel transform is performed to suppress the contributions from high excited states. The hadron masses and coupling constants are obtained as

$$\begin{aligned} m_{\mp}^2(s_0, M_B^2) &= \frac{\int_{s_<}^{s_0} [\sqrt{s} \rho_{\not{p}}^{\text{OPE}}(s) \pm \rho_I^{\text{OPE}}(s)] s e^{-s/M_B^2} ds}{\int_{s_<}^{s_0} [\sqrt{s} \rho_{\not{p}}^{\text{OPE}}(s) \pm \rho_I^{\text{OPE}}(s)] e^{-s/M_B^2} ds} \end{aligned} \quad (16)$$

and

$$\begin{aligned} f_{\mp}^2(s_0, M_B) &= \frac{\int_{s_<}^{s_0} [\sqrt{s} \rho_{\not{p}}^{\text{OPE}}(s) \pm \rho_I^{\text{OPE}}(s)] e^{-s/M_B^2} ds}{2m_{\mp}} \times e^{m_{\mp}^2/M_B^2}, \end{aligned} \quad (17)$$

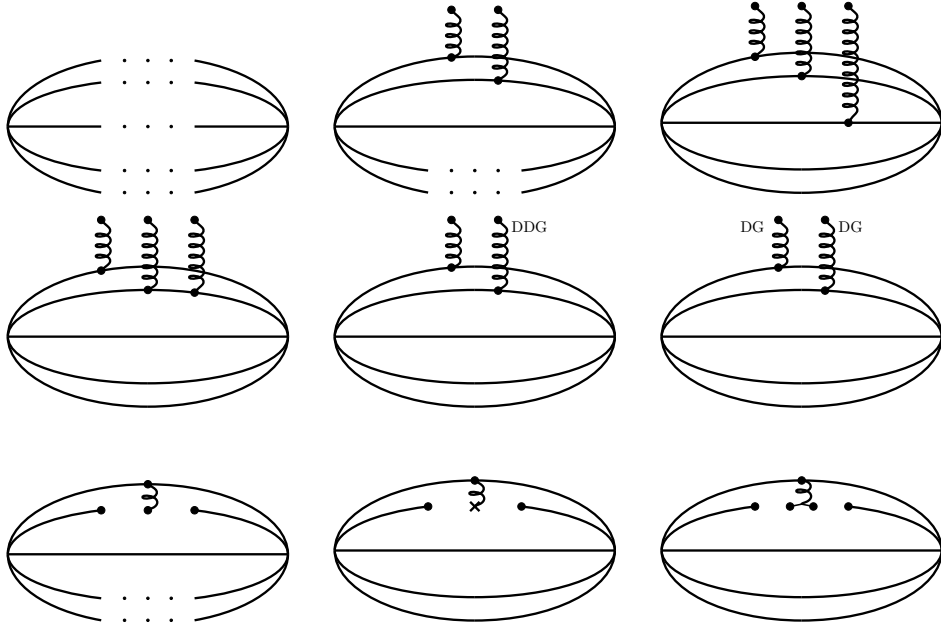


FIG. 1: The Feynman diagrams involved in our calculations for the $\Xi(1530)K$ molecular pentaquark state. A quark line with dots contains terms proportional to the color factor δ^{ij} in the propagator $S^{ij}(x)$; consequently, such diagrams effectively subsume multiple Feynman diagrams.

which are functions of the Borel parameter M_B and continuum threshold s_0 .

In the following analysis, we employ the same two-point QCD sum rule approach to determine the ground-state Ξ baryon mass and its coupling constant f_Ξ appearing in Eq. (20).

C. Three-point correlation function

In QCD sum rules, the three-point correlation function is used to study the strong decay properties of hadrons. It is defined as

$$\begin{aligned} \Pi_{\mu\nu}(p_1^2, p_2^2, p^2) &\equiv \int d^d x d^d y e^{ip_1 \cdot x} e^{ip_2 \cdot y} \Gamma(x, y), \\ \Gamma(x, y) &\equiv \langle 0 | T [J_\Xi(x) J_K(y) \bar{J}_\mu(0)] | 0 \rangle, \end{aligned} \quad (18)$$

where J_Ξ denotes the interpolating current associated with the Ξ baryon

$$J_\Xi(x) = \epsilon^{abc} [s^{aT}(x) C \gamma_\mu s^b(x)] \gamma^\mu \gamma^5 d^c(x). \quad (19)$$

The currents J_Ξ and J_K couple to the physical states $|\Xi; 1/2^+\rangle$ and $|K; 0^-\rangle$ respectively, through the following matrix elements

$$\begin{aligned} \langle 0 | J_\Xi | \Xi; 1/2^+ \rangle &= f_\Xi u(p_1), \\ \langle 0 | J_K | K; 0^- \rangle &= \frac{f_K m_K}{m_s + m_d} \equiv \lambda_K. \end{aligned} \quad (20)$$

The interaction among the Ω^* , Ξ , and K hadrons is described by the effective Lagrangian [78]

$$\mathcal{L}_{K\Xi\Omega^*} = ig_{\Omega^*\Xi K} \bar{\Xi} \gamma^{\mu\nu\lambda} \gamma^5 (\partial_\mu \Omega_\nu^*) \partial_\lambda K + h.c.. \quad (21)$$

After inserting complete set of intermediate hadronic states, the phenomenological representation of the three-point correlation function can be written as

$$\begin{aligned} \Pi_{\mu\nu}(p_1^2, p_2^2, p^2) &= \\ &\frac{\lambda_K f_\Xi u(p_1) \langle K(p_2) \Xi(p_1) | \Omega^*(p_1) \rangle f_- \bar{u}_\mu(p)}{(p^2 - m_{\Omega^*}^2 + i\epsilon)(p_1^2 - m_\Xi^2 + i\epsilon)(p_2^2 - m_K^2 + i\epsilon)} + \dots, \end{aligned} \quad (22)$$

where the “...” contains the contributions of higher excited states. The transition matrix element can be derived from the effective Lagrangian in Eq. (21) as

$$\langle K(p_2) \Xi(p_1) | \Omega^*(p) \rangle = \bar{u}(p_1) ig_{\Omega^*\Xi K} \gamma^{\mu\nu\lambda} \gamma^5 p_2^\lambda p_1^\mu u_\nu(p). \quad (23)$$

Substituting Eq. (23) into Eq. (22), we obtain

$$\begin{aligned} \Pi_{\mu\nu}(p_1^2, p_2^2, p^2) &= \\ &= \frac{ig_{\Omega^*\Xi K} \lambda_K f_\Xi f_- m_\Xi p_2^\lambda \not{p}_1 \gamma^\mu \gamma^5}{3(p^2 - m_{\Omega^*}^2 + i\epsilon)(p_1^2 - m_\Xi^2 + i\epsilon)(p_2^2 - m_K^2 + i\epsilon)} \\ &+ \dots \end{aligned} \quad (24)$$

In view of the complexity of the full expression, we keep only the Lorentz structure $\not{p}_1 \gamma^\mu \gamma^5$ in Eq. (24) for the convenience of subsequent analysis.

This result can be equivalently rewritten as

$$\begin{aligned} & \Pi_{\mu\nu}(p_1^2, p_2^2, p^2) \\ & \left(1 + \frac{m_K^2}{p_2^2 - m_K^2 + i\varepsilon}\right) \frac{\frac{1}{3}m_{\Xi}ig_{\Omega^*\Xi K}\lambda_K f_{\Xi}f_-}{(p^2 - m_{\Omega^*}^2 + i\varepsilon)(p_1^2 - m_{\Xi}^2 + i\varepsilon)} \\ & + \dots \end{aligned} \quad (25)$$

To properly apply the sum rules, we isolate the terms proportional to $1/p_2^2$ with the Lorentz structure $\not{p}_1 \gamma^\mu \gamma^5$ in the OPE series. This procedure determines the coupling constant $g_{\Omega^*\Xi K}(Q^2)$ (where $Q^2 = -p_2^2$) in a region away from the physical pole at $Q^2 = -m_K^2$. The on-shell coupling is then obtained by extrapolating from the valid QCD sum rule window. By equating the hadronic and OPE representations and assuming $p^2 = p_1^2$, we have

$$\begin{aligned} & \frac{m_K^2}{(p_2^2 - m_K^2 + i\varepsilon)} \frac{\frac{1}{3}m_{\Xi}ig_{\Omega^*\Xi K}\lambda_K f_{\Xi}f_-}{(p^2 - m_{\Omega^*}^2 + i\varepsilon)(p^2 - m_{\Xi}^2 + i\varepsilon)} + \dots \\ & = \frac{1}{p_2^2} \left[\int_0^{s_0} ds \frac{\rho(s)}{s - p^2} + \int_{s_0}^{\infty} ds \frac{\rho(s)}{s - p^2} \right]. \end{aligned} \quad (26)$$

According to quark-hadron duality, the contributions from higher resonances and the continuum on the phenomenological side are assumed to be dual to the integral above the continuum threshold s_0 on the OPE side. After performing the Borel transform, the sum rules are obtained as

$$\begin{aligned} & \frac{1}{3}m_{\Xi}m_K^2ig_{\Omega^*\Xi K}\lambda_K f_{\Xi}f_- \frac{Q^2 + m_K^2}{Q^2} \frac{e^{-m_{\Omega^*}^2/M_B^2} - e^{-m_{\Xi}^2/M_B^2}}{m_{\Omega^*}^2 - m_{\Xi}^2} \\ & = \int_0^{s_0} ds \rho(s) e^{-s/M_B^2}. \end{aligned} \quad (27)$$

To extract the value of the coupling constant at the physical point $Q^2 = -m_K^2$, we extrapolate $g_{\Omega^*\Xi K}(Q^2)$ from the working region of QCD sum rules by using an exponential model [79–81]

$$g_{\Omega^*\Xi K}(Q^2) = g_1 e^{-g_2 Q^2}, \quad (28)$$

where the parameters g_1 and g_2 are determined by fitting the numerical results obtained from the sum rules.

The decay width of the process $\Omega^* \rightarrow \Xi K$ can be derived from Eq. (21) as

$$\begin{aligned} \Gamma(\Omega^* \rightarrow \Xi K) & = \frac{\sqrt{\lambda(m_{\Omega^*}^2, m_{\Xi}^2, m_K^2)}}{192\pi m_{\Omega^*}^3} g_{\Omega^*\Xi K}^2 \\ & \times (m_{\Omega^*}^2 - 2m_{\Omega^*}m_{\Xi} - m_K^2 + m_{\Xi}^2)^2 \\ & \times (m_{\Omega^*}^2 + 2m_{\Omega^*}m_K - m_K^2 + m_{\Xi}^2), \end{aligned} \quad (29)$$

where λ is the well-known Källén function

$$\lambda(a, b, c) = a^2 + b^2 + c^2 - 2ab - 2ac - 2bc. \quad (30)$$

At the quark–gluon level, we evaluate the three-point correlation function using the same light-quark propagators given in Eq. (14). We preserve the spectral function $\rho^{\text{OPE}}(s)$ up to dimension 10 and the corresponding Feynman diagrams are shown in Fig. 2. The result of $\rho(s)$ is obtained as

$$\begin{aligned} \rho^{\text{OPE}}(s) & = \frac{5\langle g^2 G^2 \rangle}{98304\pi^6} s^2 + \frac{5m_s \langle \bar{s}s \rangle}{6144\pi^4} s^2 - \frac{5m_s \langle \bar{q}q \rangle}{3072\pi^4} s^2 \\ & - \frac{7g^2 \langle \bar{s}s \rangle^2}{41472\pi^4} s - \frac{7g^2 \langle \bar{q}q \rangle^2}{41472\pi^4} s - \frac{7\langle g^3 f G^3 \rangle}{2^{15} \times 3^3 \times \pi^6} s \\ & - \frac{7m_s \langle \bar{s}g\sigma Gs \rangle}{18432\pi^4} s + \frac{m_s \langle \bar{q}g\sigma Gq \rangle}{1536\pi^4} s \\ & - \frac{55m_s \langle \bar{s}s \rangle \langle g^2 G^2 \rangle}{12288\pi^4} + \frac{5m_s \langle \bar{q}q \rangle \langle g^2 G^2 \rangle}{6144\pi^4}. \end{aligned} \quad (31)$$

III. NUMERICAL ANALYSES

A. The mass of $\Xi(1530)K$ molecular pentaquark

For the numerical analyses, we adopt values of the QCD parameters at the renormalization scale $\mu = 1$ GeV with $\Lambda_{\text{QCD}} = 300$ MeV, which are standard in QCD sum rule calculations [41, 74, 82–89]

$$\begin{aligned} m_u & = m_d = 0, m_s = 93.5 \pm 0.8 \text{ MeV}, \\ \langle \bar{q}q \rangle & = -(0.24 \pm 0.01)^3 \text{ GeV}^3, \\ \langle \bar{s}s \rangle & = (0.8 \pm 0.1) \langle \bar{q}q \rangle, \\ \langle \bar{q}g\sigma Gq \rangle & = (0.8 \pm 0.2) \langle \bar{q}q \rangle \text{ GeV}^2, \\ \langle g^2 G^2 \rangle & = (0.48 \pm 0.14) \text{ GeV}^4, \\ \langle g^3 f G^3 \rangle & = (8.2 \pm 1) \langle \alpha_s G^2 \rangle \text{ GeV}^2. \end{aligned} \quad (32)$$

Here the strange quark mass is taken at the renormalization scale $\mu = 2$ GeV. The renormalization group equation is used to evolve m_s to the working scale $\mu = 1$ GeV.

We begin by examining the behavior of the spectral function before proceeding to the mass sum rule analysis. As illustrated in Fig. 3, the spectral density suffers from poor positivity, becoming negative over a relatively wide region, $1 \text{ GeV}^2 \leq s \leq 4 \text{ GeV}^2$. To remedy this unphysical behavior, we relax the factorization assumption by introducing a parameter κ via $\langle \bar{q}q q q \rangle = \kappa \langle \bar{q}q \rangle^2$ [89–91]. With $\kappa = 1.70$, the spectral density exhibits sufficiently good behavior, which will be adopted in the following analysis.

In Eq. (16), the extracted hadron mass depends on two free parameters: the Borel parameter M_B^2 and continuum threshold s_0 . Their working regions are determined by imposing the following standard criteria: (a) good convergence of the operator product expansion, (b) a sufficiently large pole contribution, and (c) good stability of the mass sum rules.

The convergence of the OPE is quantified by requiring that the contributions from high-dimensional operators

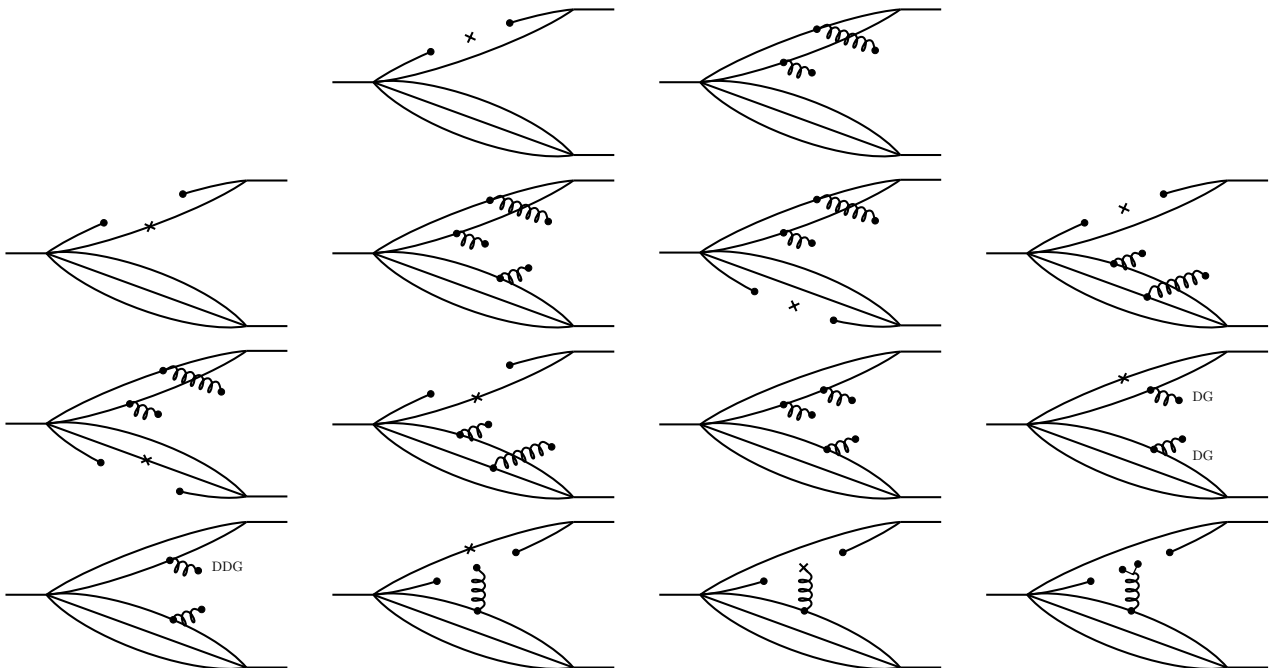


FIG. 2: The Feynman diagrams which contribute to the theoretical side of the three-point sum rules in the relevant structure for the two-body strong decays of $\Xi(1530)K$ molecular pentaquark state.

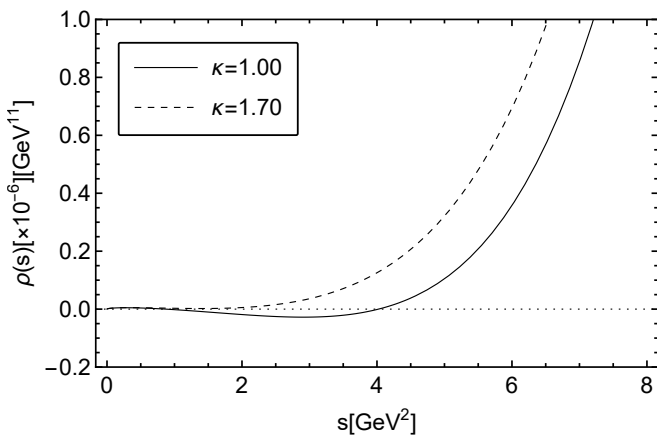


FIG. 3: Behaviors of the spectral densities for different factorization assumption. The solid lines represent the spectral densities for $\kappa = 1$, whereas the dashed lines are the corresponding densities considering $\kappa = 1.70$.

be sufficiently suppressed

$$\text{CVG} \equiv \left| \frac{\Pi_-^{8+9+10}(\infty, M_B^2)}{\Pi_-(\infty, M_B^2)} \right| \leq 10\%, \quad (33)$$

where Π_- denotes the full OPE series of correlation function, while Π_-^{8+9+10} represents the combined contributions from the dimension-8, 9, and 10 condensates. As shown in Fig. 4, this requirement leads to a lower bound on the Borel parameter $M_B^2 \geq 2.74 \text{ GeV}^2$.

To determine the optimal value of the continuum

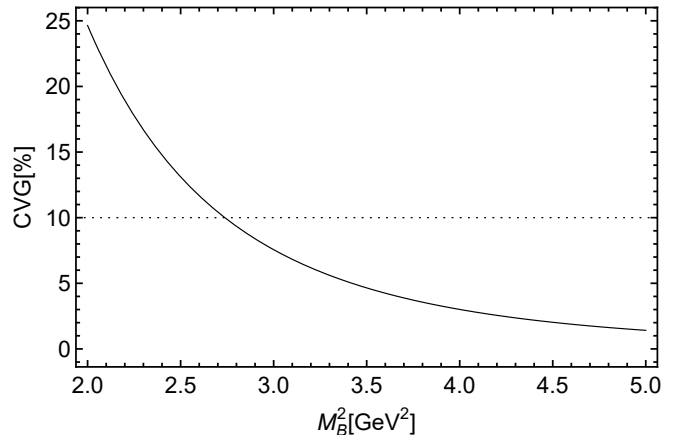


FIG. 4: OPE convergence for the $\Xi(1530)K$ molecular pentaquark state considering $\kappa = 1.70$.

threshold s_0 , we plot the m_H-s_0 curves for different values of M_B^2 in Fig. 5. The optimal s_0 is chosen such that the dependence of m_H on M_B^2 is minimized in its vicinity. To quantify this criterion, we define the function χ^2 as [92–94]

$$\chi^2(s_0) = \sum_{i=1}^N \left[\frac{m_H(s_0, M_{B,i}^2)}{\bar{m}_H(s_0)} - 1 \right]^2, \quad (34)$$

where $\bar{m}_H(s_0)$ denotes the average value of the data

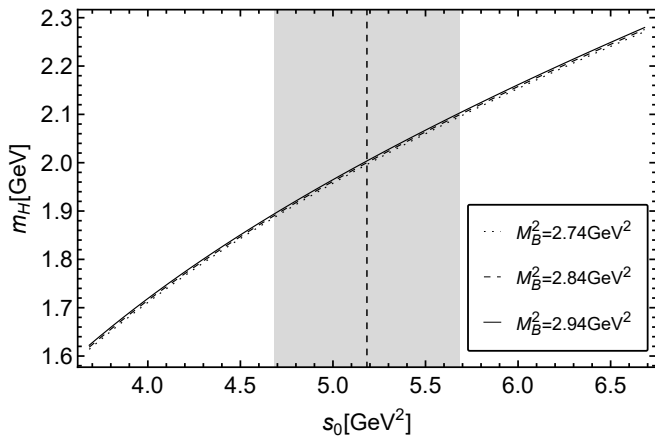


FIG. 5: Variation of hadron mass with s_0 corresponding to the $\Xi(1530)K$ molecular pentaquark state considering $\kappa = 1.70$.

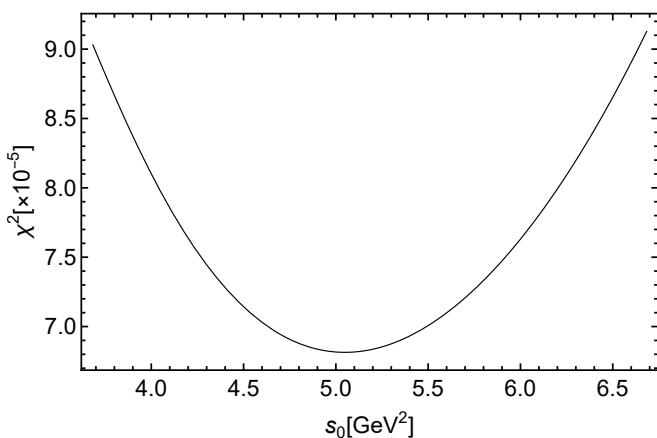


FIG. 6: Variation of χ^2 with s_0 corresponding to the $\Xi(1530)K$ molecular pentaquark state considering $\kappa = 1.70$.

points

$$\bar{m}_H(s_0) = \sum_{i=1}^N \frac{m_H(s_0, M_{B,i}^2)}{N}. \quad (35)$$

The χ^2 as a function of s_0 is shown in Fig. 6, from which the optimal value of the continuum threshold is determined from the location of the minimum as $s_0 = 5.18$ GeV².

In addition, for a sufficient pole contribution we require

$$\text{PC} \equiv \left| \frac{\Pi_-(s_0, M_B^2)}{\Pi_-(\infty, M_B^2)} \right| \geq 2\%. \quad (36)$$

Applying the above constraints yields an acceptable Borel window of $2.74 \text{ GeV}^2 \leq M_B^2 \leq 2.94 \text{ GeV}^2$. The corresponding Borel curves are displayed in Fig. 7, where the extracted mass exhibits good stability against variations of M_B^2 within this window. As a result, we obtain the mass and coupling constant of the $\Xi(1530)K$ molec-

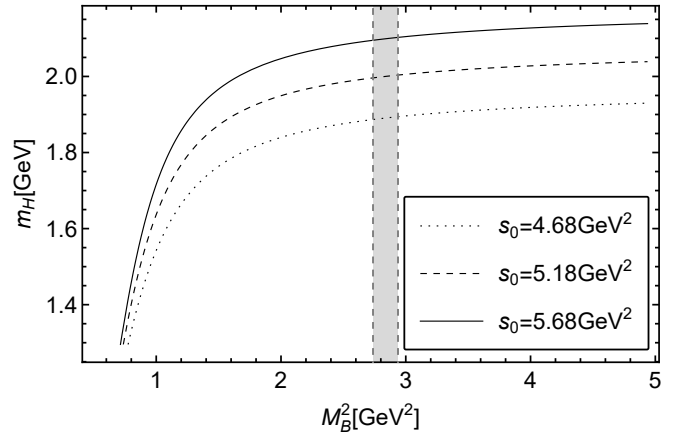


FIG. 7: Variation of hadron mass with M_B^2 corresponding to the $\Xi(1530)K$ molecular pentaquark state considering $\kappa = 1.70$.

ular state as

$$m_{\Xi(1530)K} = 2.00 \pm 0.15 \text{ GeV}, \quad (37)$$

$$f_- = (2.96 \pm 1.43) \times 10^{-4} \text{ GeV}^6, \quad (38)$$

where the errors are mainly from the uncertainties of the various condensates in Eq. (32). The extracted mass of the $\Xi(1530)K$ molecular pentaquark state is consistent with the mass of $\Omega(2012)$ collected in PDG [41].

B. The coupling constant of Ξ

To calculate the coupling constant of Ξ , we perform the mass sum rule analysis for the current in Eq. (19) and adopt the same values of the QCD parameters in Eq. (32). Under the following constraints

$$\begin{aligned} \text{CVG} &\equiv \left| \frac{\Pi_-^{6+7+8}(\infty, M_B^2)}{\Pi_-(\infty, M_B^2)} \right| \leq 1\%, \\ \text{PC} &\equiv \left| \frac{\Pi_-(s_0, M_B^2)}{\Pi_-(\infty, M_B^2)} \right| \geq 20\%, \end{aligned} \quad (39)$$

the acceptable Borel window is determined to be $2.61 \text{ GeV}^2 \leq M_B^2 \leq 3.41 \text{ GeV}^2$. The corresponding Borel curves are shown in Fig. 8. As a result, we obtain the mass and coupling constant of Ξ as

$$m_{\Xi} = 1.32 \pm 0.06 \text{ GeV}, \quad (40)$$

$$f_{\Xi} = (2.74 \pm 0.40) \times 10^{-2} \text{ GeV}^3, \quad (41)$$

in which the obtained mass agrees well with the mass of Ξ baryon with $J^P = 1/2^+$ in PDG [41].

C. The strong decays of $\Omega(2012) \rightarrow \Xi^0 K^-$ and $\Xi^- K^0$

To perform the three-point sum rule analyses, we adopt the input parameters listed in Eq. (32) and the same fac-

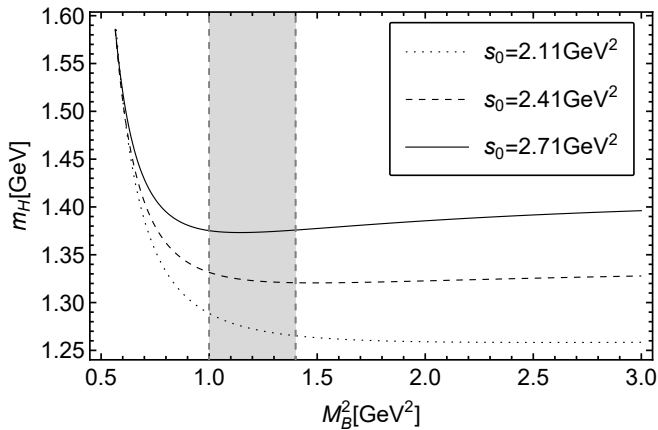


FIG. 8: Variation of hadron mass with M_B^2 corresponding to the Ξ state.

torization parameter $\kappa = 1.70$. For the Ξ and K doublets and $\Omega(2012)$, we use the hadron parameter values from PDG [41]:

$$\begin{aligned}
 m_{\Omega(2012)} &= 2012.4 \pm 0.9 \text{ MeV}, \\
 m_{\Xi^-} &= 1321.71 \pm 0.07 \text{ MeV}, \\
 m_{\Xi^0} &= 1314.86 \pm 0.20 \text{ MeV}, \\
 m_{K^0} &= 497.611 \pm 0.013 \text{ MeV}, \\
 m_{K^-} &= 493.677 \pm 0.015 \text{ MeV}, \\
 f_K &= 155.7 \text{ MeV}.
 \end{aligned} \tag{42}$$

As shown in Eq. (27), the coupling constant extracted from the sum rule depends on the s_0 and M_B^2 in the limit $Q^2 \rightarrow 0$. Adopting the same value of $s_0 = 5.18 \text{ GeV}^2$ in the mass sum rule, we present the dependence of the coupling constant on M_B^2 at the Euclidean momentum point $Q^2 = m_{\Xi^-}^2$ in Fig. 9. We find that the sum rules yield a stable platform for the coupling constant at $M_B^2 \sim 0.72 \text{ GeV}^2$, around which it has minimal parameter dependence.

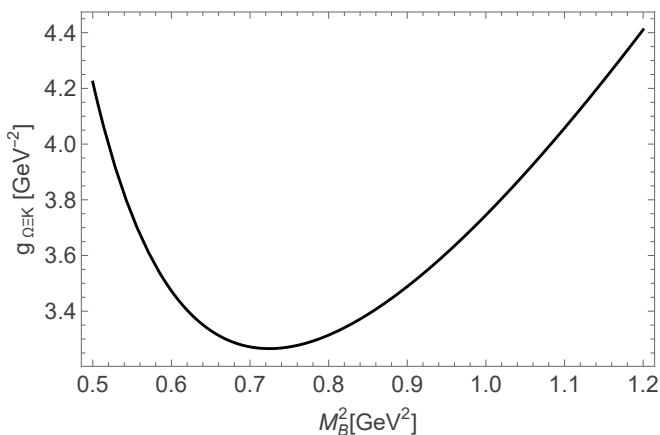


FIG. 9: Variation of the coupling constant $g_{\Omega^* \Xi^- K^0}(Q^2 = m_{\Xi^-}^2)$ with the Borel parameter M_B^2 for $s_0 = 5.18 \text{ GeV}^2$.

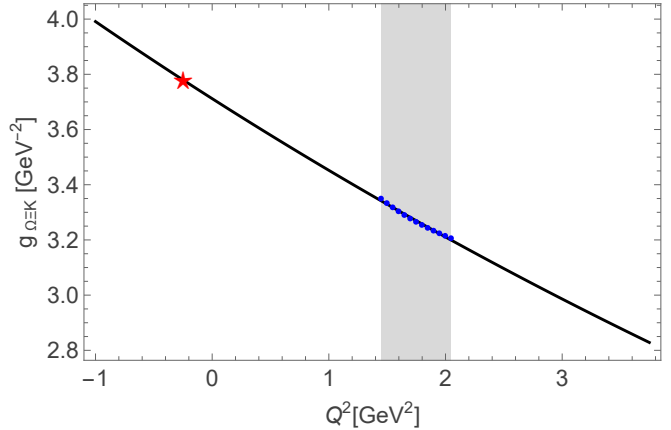


FIG. 10: Variation of the coupling constant $g_{\Omega^* \Xi^- K^0}$ with Q^2 . The dotted points represent the QCD sum rules results for $g_{\Omega^* \Xi^- K^0}$ with $s_0 = 5.18 \text{ GeV}^2$ and $M_B^2 = 0.72 \text{ GeV}^2$. The solid line is the fit of the QCD sum rules result through model Eq. (28) and the extrapolation to the physical pole $Q^2 = -m_{K^0}^2$.

To extract the value of the coupling constant at the physical point $Q^2 = -m_{K^0}^2$, we extrapolate $g_{\Omega^* \Xi^- K^0}(Q^2)$ from the QCD sum rules working region using the exponential model given in Eq. (28). As shown in Fig. 10, the QCD sum rules results obtained with $s_0 = 5.18 \text{ GeV}^2$ and $M_B^2 = 0.72 \text{ GeV}^2$ are well described by this model, yielding the fitted parameters $g_1 = 3.71 \text{ GeV}^{-1}$ and $g_2 = 0.07 \text{ GeV}^{-2}$. Using these parameters, the coupling constant at $Q^2 = -m_{K^0}^2$ is obtained as

$$g_{\Omega^* \Xi^- K^0} = 3.78_{-1.65}^{+3.74} \text{ GeV}^{-2}, \tag{43}$$

where the errors are mainly from the uncertainties of the coupling constant in Eqs. (38) and (41), the various condensates in Eq. (32), and the hadron parameter values in Eq. (42).

According to Eq. (29), the partial decay width of the process $\Omega(2012) \rightarrow \Xi^- K^0$ can be calculated as

$$\Gamma(\Omega^* \rightarrow \Xi^- K^0) = 1.82_{-1.24}^{+5.39} \text{ MeV}. \tag{44}$$

For the $\Omega(2012) \rightarrow \Xi^0 K^-$ decay, the only difference comes from the isospin mass-splitting of the Ξ and K doublets in the final states. Following the same procedure, we obtain the fitted parameters $g_1 = 3.77 \text{ GeV}^{-1}$ and $g_2 = 0.07 \text{ GeV}^{-2}$ in the extrapolation model. With these values, the coupling constant at $Q^2 = -m_{K^-}^2$ and the corresponding partial decay width are determined to be

$$g_{\Omega^* \Xi^0 K^-} = 3.84_{-1.68}^{+3.78} \text{ GeV}^{-2}, \tag{45}$$

$$\Gamma(\Omega^* \rightarrow \Xi^0 K^-) = 2.15_{-1.47}^{+6.33} \text{ MeV}. \tag{46}$$

As a result, the total two-body decay width and its branching fraction for the $\Xi^* K$ molecular pentaquark

state are

$$\Gamma(\Omega^* \rightarrow \Xi K) = 3.97_{-1.92}^{+8.31} \text{ MeV}, \quad (47)$$

$$\mathcal{B}[\Omega^* \rightarrow \Xi K] \equiv \frac{\Gamma(\Omega^* \rightarrow \Xi K)}{\Gamma_{total}^{exp}} \approx 0.62, \quad (48)$$

in which $\Gamma_{total}^{exp} = 6.4_{-2.6}^{+3.0}$ MeV is the experimental total decay width of $\Omega(2012)$. The result of the branching fraction for the two-body decays agrees well with recent experimental data $\mathcal{B}[\Omega^* \rightarrow \Xi K] = 0.62_{-0.17}^{+0.27}$ from the ALICE Collaboration in 2025 [39]. The branching fraction ratio of the two-body decays is obtained as

$$\begin{aligned} \mathcal{R}_{\Xi^0 K^-}^{\Xi^- K^0} &\equiv \frac{\mathcal{B}[\Omega(2012) \rightarrow \Xi^- K^0]}{\mathcal{B}[\Omega(2012) \rightarrow \Xi^0 K^-]} \\ &= \frac{\Gamma(\Omega^* \rightarrow \Xi^- K^0)}{\Gamma(\Omega^* \rightarrow \Xi^0 K^-)} \approx 0.85, \end{aligned} \quad (49)$$

which is also in good agreement with the experimental data collected in PDG [41].

Under the assumption that all $\Omega(2012)$ decays are either $\Omega(2012) \rightarrow \Xi K$ or $\Omega(2012) \rightarrow \Xi \pi K$, we can also estimate the relative branching fraction between the decays of the three-body $\Omega(2012) \rightarrow \Xi \pi K$ and two-body $\Omega(2012) \rightarrow \Xi K$ as

$$\begin{aligned} \mathcal{R}_{\Xi K}^{\Xi \pi K} &\equiv \frac{\mathcal{B}[\Omega^* \rightarrow \Xi(1530)K \rightarrow \Xi \pi K]}{\mathcal{B}[\Omega^* \rightarrow \Xi K]} \\ &= \frac{\Gamma_{total}^{exp} - \Gamma(\Omega^* \rightarrow \Xi K)}{\Gamma(\Omega^* \rightarrow \Xi K)} \approx 0.61. \end{aligned} \quad (50)$$

This estimated ratio is in good agreement with the result reported by the ALICE Collaboration under the same assumption in 2025 [39], and is also roughly consistent with the experimental value $\mathcal{R}_{\Xi K}^{\Xi \pi K} = 0.99 \pm 0.26 \pm 0.06$ reported by the Belle Collaboration in 2022 [72].

IV. CONCLUSION AND DISCUSSION

In this work, we have investigated the recently observed $\Omega(2012)$ as a $\Xi(1530)K$ molecular pentaquark

state within the framework of QCD sum rules. We construct the unique molecular interpolating current with $IJ^P = 0\frac{3}{2}^-$ and calculate the correlation functions by employing the parity-projected sum rules to separate the positive- and negative-parity contributions. We calculate the two-point correlation function to investigate the hadron mass and the three-point correlation function to study the two-body strong decay properties of the $\Xi(1530)K$ pentaquark state.

Our QCD sum rule analyses yield a mass of 2.00 ± 0.15 GeV for the $\Xi(1530)K$ molecular pentaquark state, a total two-body decay width of $\Gamma(\Omega^* \rightarrow \Xi K) = 3.97_{-1.92}^{+8.31}$ MeV and branching fraction $\mathcal{B}[\Omega^* \rightarrow \Xi K] = 0.62$. The branching fraction ratio of the two-body decay channels is obtained as $\mathcal{R}_{\Xi^0 K^-}^{\Xi^- K^0} = 0.85$. These results are in excellent agreement with the experimental data for $\Omega(2012)$, providing strong evidence for its interpretation as a $\Xi(1530)K$ molecular pentaquark state. Moreover, we estimate the ratio of the three-body to two-body decays branching fractions as $\mathcal{R}_{\Xi K}^{\Xi \pi K} = 0.61$, which is consistent with the result reported by the ALICE Collaboration in 2025, and is also in rough agreement with the measurement of Belle in 2022. These calculations are useful for providing further insight into the internal structure of $\Omega(2012)$ in the future.

Acknowledgments

This work is supported by the National Natural Science Foundation of China under Grant No. 12575153.

Appendix A: The spectral densities for the negative-parity $\Xi(1530)K$ molecular state

The explicit expressions for the spectral densities $\rho_p^{\text{OPE}}(s)$ and $\rho_I^{\text{OPE}}(s)$ are presented in Eqs. (A1) and (A2), respectively.

$$\begin{aligned}
\rho_{\not{p}}^{\text{OPE}}(s) = & \frac{s^5}{15728640\pi^8} + \frac{31\langle\bar{s}s\rangle m_s s^3}{737280\pi^6} - \frac{13\langle\bar{q}q\rangle m_s s^3}{92160\pi^6} + \frac{61\langle g^2 G^2 \rangle s^3}{212336640\pi^8} + \frac{251\langle\bar{q}g\sigma Gq\rangle m_s s^2}{368640\pi^6} \\
& + \frac{\langle\bar{s}g\sigma Gs\rangle m_s s^2}{6144\pi^6} - \frac{g^2\langle\bar{q}q\rangle^2 s^2}{41472\pi^6} - \frac{83g^2\langle\bar{s}s\rangle^2 s^2}{622080\pi^6} - \frac{\langle\bar{q}q\rangle^2 s^2}{4608\pi^4} + \frac{7\langle\bar{s}s\rangle^2 s^2}{11520\pi^4} + \frac{\langle\bar{q}q\rangle\langle\bar{s}s\rangle s^2}{360\pi^4} \\
& - \frac{23\langle g^3 G^3 \rangle s^2}{5308416\pi^8} - \frac{35\langle g^2 G^2 \rangle\langle\bar{q}q\rangle m_s s}{110592\pi^6} - \frac{329\langle g^2 G^2 \rangle\langle\bar{s}s\rangle m_s s}{589824\pi^6} + \frac{\langle\bar{q}q\rangle\langle\bar{q}g\sigma Gq\rangle s}{4608\pi^4} \\
& - \frac{37\langle\bar{q}q\rangle\langle\bar{s}g\sigma Gs\rangle s}{4608\pi^4} - \frac{49\langle\bar{s}s\rangle\langle\bar{q}g\sigma Gq\rangle s}{6912\pi^4} - \frac{143\langle\bar{s}s\rangle\langle\bar{s}g\sigma Gs\rangle s}{27648\pi^4} - \frac{\langle\bar{q}q\rangle\langle\bar{s}g\sigma Gs\rangle m_s^2}{864\pi^4} \\
& - \frac{91\langle\bar{s}s\rangle\langle\bar{s}g\sigma Gs\rangle m_s^2}{6912\pi^4} + \frac{2405\langle g^2 G^2 \rangle\langle\bar{s}g\sigma Gs\rangle m_s}{5308416\pi^6} + \frac{985\langle g^2 G^2 \rangle\langle\bar{q}g\sigma Gq\rangle m_s}{5308416\pi^6} + \frac{\langle\bar{s}s\rangle^3 m_s}{96\pi^2} \\
& - \frac{13\langle\bar{q}q\rangle^2\langle\bar{s}s\rangle m_s}{96\pi^2} - \frac{5g^2\langle\bar{q}q\rangle^2\langle\bar{s}s\rangle m_s}{1152\pi^4} + \frac{5g^2\langle\bar{q}q\rangle\langle\bar{s}s\rangle^2 m_s}{1296\pi^4} - \frac{11g^2\langle\bar{s}s\rangle^3 m_s}{1944\pi^4} \\
& - \frac{g^2\langle\bar{q}q\rangle^3 m_s}{2592\pi^4} + \frac{11\langle g^3 G^3 \rangle\langle\bar{q}q\rangle m_s}{24576\pi^6} + \frac{113\langle g^3 G^3 \rangle\langle\bar{s}s\rangle m_s}{147456\pi^6} - \frac{11g^2\langle g^2 G^2 \rangle\langle\bar{q}q\rangle^2}{2239488\pi^6} \\
& - \frac{\langle g^2 G^2 \rangle\langle\bar{q}q\rangle^2}{6912\pi^4} + \frac{11\langle g^2 G^2 \rangle\langle\bar{s}s\rangle^2}{9216\pi^4} + \frac{41\langle g^2 G^2 \rangle\langle\bar{s}s\rangle^2}{8957952\pi^6} \\
& + \frac{11\langle g^2 G^2 \rangle\langle\bar{q}q\rangle\langle\bar{s}s\rangle}{13824\pi^4} + \frac{193\langle\bar{q}g\sigma Gq\rangle\langle\bar{s}g\sigma Gs\rangle}{27648\pi^4} + \frac{5\langle\bar{q}g\sigma Gq\rangle^2}{27648\pi^4} + \frac{3\langle\bar{s}g\sigma Gs\rangle^2}{1024\pi^4}.
\end{aligned} \tag{A1}$$

$$\begin{aligned}
\rho_I^{\text{OPE}}(s) = & \frac{3m_s s^5}{5734400\pi^8} - \frac{\langle\bar{s}s\rangle s^4}{49152\pi^6} - \frac{\langle\bar{q}q\rangle s^4}{110592\pi^6} + \frac{7\langle\bar{q}g\sigma Gq\rangle s^3}{92160\pi^6} + \frac{47\langle\bar{s}g\sigma Gs\rangle s^3}{276480\pi^6} \\
& + \frac{79\langle g^2 G^2 \rangle m_s s^3}{8847360\pi^8} + \frac{23\langle\bar{s}g\sigma Gs\rangle m_s^2 s^2}{36864\pi^6} + \frac{\langle\bar{q}q\rangle^2 m_s s^2}{768\pi^4} - \frac{\langle\bar{s}s\rangle^2 m_s s^2}{128\pi^4} \\
& + \frac{13\langle\bar{q}q\rangle\langle\bar{s}s\rangle m_s s^2}{768\pi^4} + \frac{13g^2\langle\bar{q}q\rangle^2 m_s s^2}{165888\pi^6} - \frac{7g^2\langle\bar{s}s\rangle^2 m_s s^2}{995328\pi^6} - \frac{799\langle g^3 G^3 \rangle m_s s^2}{21233664\pi^8} \\
& - \frac{25\langle g^2 G^2 \rangle\langle\bar{q}q\rangle s^2}{442368\pi^6} - \frac{71\langle g^2 G^2 \rangle\langle\bar{s}s\rangle s^2}{442368\pi^6} + \frac{\langle\bar{s}s\rangle^3 s}{216\pi^2} - \frac{17\langle\bar{q}q\rangle\langle\bar{s}s\rangle s}{216\pi^2} \\
& - \frac{7\langle\bar{q}q\rangle^2\langle\bar{s}s\rangle s}{864\pi^2} + \frac{g^2\langle\bar{s}s\rangle^3 s}{11664\pi^4} - \frac{g^2\langle\bar{q}q\rangle^2\langle\bar{s}s\rangle s}{2592\pi^4} - \frac{5g^2\langle\bar{q}q\rangle^3 s}{3888\pi^4} + \frac{7g^2\langle\bar{q}q\rangle\langle\bar{s}s\rangle s}{3888\pi^4} \\
& + \frac{\langle g^3 G^3 \rangle\langle\bar{q}q\rangle s}{6144\pi^6} + \frac{67\langle g^3 G^3 \rangle\langle\bar{s}s\rangle s}{248832\pi^6} + \frac{341\langle g^2 G^2 \rangle\langle\bar{q}g\sigma Gq\rangle s}{5308416\pi^6} \\
& + \frac{1067\langle g^2 G^2 \rangle\langle\bar{s}g\sigma Gs\rangle s}{5308416\pi^6} + \frac{29\langle\bar{s}s\rangle\langle\bar{s}g\sigma Gs\rangle m_s s}{1728\pi^4} - \frac{85\langle\bar{q}q\rangle\langle\bar{s}g\sigma Gs\rangle m_s s}{2304\pi^4} \\
& - \frac{41\langle\bar{q}q\rangle\langle\bar{q}g\sigma Gq\rangle m_s s}{4608\pi^4} - \frac{149\langle\bar{s}s\rangle\langle\bar{q}g\sigma Gq\rangle m_s s}{6912\pi^4}.
\end{aligned} \tag{A2}$$

- [1] M. Gell-Mann, Phys. Lett. **8**, 214 (1964)
[2] G. Zweig, An SU(3) model for strong interaction symmetry and its breaking. Version 2, 22–101 (1964)
[3] C. A. Meyer and E. S. Swanson, Prog. Part. Nucl. Phys. **82**, 21 (2015)
[4] H.-X. Chen, W. Chen, X. Liu, and S.-L. Zhu, Phys. Rept. **639**, 1 (2016)
[5] H. Clement, Prog. Part. Nucl. Phys. **93**, 195 (2017)
[6] F.-K. Guo, C. Hanhart, U.-G. Meißner, Q. Wang, Q. Zhao, and B.-S. Zou, Rev. Mod. Phys. **90**, 015004 (2018), [Erratum: Rev.Mod.Phys. 94, 029901 (2022)]
[7] Y.-R. Liu, H.-X. Chen, W. Chen, X. Liu, and S.-L. Zhu, Prog. Part. Nucl. Phys. **107**, 237 (2019)
[8] N. Brambilla et al., Phys. Rept. **873**, 1 (2020)
[9] H.-X. Chen, W. Chen, X. Liu, Y.-R. Liu, and S.-L. Zhu, Rept. Prog. Phys. **86**, 026201 (2023)
[10] M.-Z. Liu, Y.-W. Pan, Z.-W. Liu, T.-W. Wu, J.-X. Lu, and L.-S. Geng, Phys. Rept. **1108**, 1 (2025)

- [11] A. Esposito, A. Pilloni, and A. D. Polosa, *Phys. Rept.* **668**, 1 (2017)
- [12] L. Meng, B. Wang, G.-J. Wang, and S.-L. Zhu, *Phys. Rept.* **1019**, 1 (2023)
- [13] R. F. Lebed, R. E. Mitchell, and E. S. Swanson, *Prog. Part. Nucl. Phys.* **93**, 143 (2017)
- [14] A. Hosaka, T. Iijima, K. Miyabayashi, Y. Sakai, and S. Yasui, *PTEP* **2016**, 062C01 (2016)
- [15] A. Ali, J. S. Lange, and S. Stone, *Prog. Part. Nucl. Phys.* **97**, 123 (2017)
- [16] S. L. Olsen, T. Skwarnicki, and D. Zieminska, *Rev. Mod. Phys.* **90**, 015003 (2018)
- [17] Z.-G. Wang, *Front. Phys. (Beijing)* **21**, 016300 (2026)
- [18] J. Yelton et al., *Phys. Rev. Lett.* **121**, 052003 (2018)
- [19] T. M. Aliev, K. Azizi, and H. Sundu, *Eur. Phys. J. C* **77**, 222 (2017)
- [20] C. S. An and B. S. Zou, *Phys. Rev. C* **89**, 055209 (2014)
- [21] C. S. An, B. C. Metsch, and B. S. Zou, *Phys. Rev. C* **87**, 065207 (2013)
- [22] R. Bijker, F. Iachello, and A. Leviatan, *Annals Phys.* **284**, 89 (2000)
- [23] R. Bijker, J. Ferretti, G. Galatà, H. García-Tecocoatzi, and E. Santopinto, *Phys. Rev. D* **94**, 074040 (2016)
- [24] S. Capstick and N. Isgur, *Phys. Rev. D* **34**, 2809 (1986)
- [25] C. E. Carlson and C. D. Carone, *Phys. Lett. B* **484**, 260 (2000)
- [26] K.-T. Chao, N. Isgur, and G. Karl, *Phys. Rev. D* **23**, 155 (1981)
- [27] Y. Chen and B.-Q. Ma, *Nucl. Phys. A* **831**, 1 (2009)
- [28] G. P. Engel, C. B. Lang, D. Mohler, and A. Schäfer, *Phys. Rev. D* **87**, 074504 (2013)
- [29] R. N. Faustov and V. O. Galkin, *Phys. Rev. D* **92**, 054005 (2015)
- [30] J. L. Goity, C. Schat, and N. N. Scoccola, *Phys. Lett. B* **564**, 83 (2003)
- [31] C. S. Kalman, *Phys. Rev. D* **26**, 2326 (1982)
- [32] J. Liang et al., *Chin. Phys. C* **40**, 041001 (2016)
- [33] U. Loring, B. C. Metsch, and H. R. Petry, *Eur. Phys. J. A* **10**, 447 (2001)
- [34] N. Matagne and F. Stancu, *Phys. Rev. D* **74**, 034014 (2006)
- [35] Y. Oh, *Phys. Rev. D* **75**, 074002 (2007)
- [36] M. Pervin and W. Roberts, *Phys. Rev. C* **77**, 025202 (2008)
- [37] C. L. Schat, J. L. Goity, and N. N. Scoccola, *Phys. Rev. Lett.* **88**, 102002 (2002)
- [38] Y. Li et al., *Phys. Rev. D* **104**, 052005 (2021)
- [39] S. Acharya et al., *Phys. Rev. D* **112**, 092002 (2025)
- [40] M. Ablikim et al., *Phys. Rev. Lett.* **134**, 131903 (2025)
- [41] S. Navas et al., *Phys. Rev. D* **110**, 030001 (2024)
- [42] T. M. Aliev, K. Azizi, Y. Sarac, and H. Sundu, *Phys. Rev. D* **98**, 014031 (2018)
- [43] T. M. Aliev, K. Azizi, Y. Sarac, and H. Sundu, *Eur. Phys. J. C* **78**, 894 (2018)
- [44] A. J. Arifi, D. Suenaga, A. Hosaka, and Y. Oh, *Phys. Rev. D* **105**, 094006 (2022)
- [45] L. Hockley, W. Kamleh, D. Leinweber, and A. Thomas (2024)
- [46] M.-S. Liu, K.-L. Wang, Q.-F. Lü, and X.-H. Zhong, *Phys. Rev. D* **101**, 016002 (2020)
- [47] C. Menapara and A. K. Rai, *Chin. Phys. C* **46**, 103102 (2022)
- [48] M. V. Polyakov, H.-D. Son, B.-D. Sun, and A. Tandogan, *Phys. Lett. B* **792**, 315 (2019)
- [49] N. Su, H.-X. Chen, P. Gubler, and A. Hosaka, *Phys. Rev. D* **110**, 034007 (2024)
- [50] K.-L. Wang, Q.-F. Lü, J.-J. Xie, and X.-H. Zhong, *Phys. Rev. D* **107**, 034015 (2023)
- [51] Z.-Y. Wang, L.-C. Gui, Q.-F. Lü, L.-Y. Xiao, and X.-H. Zhong, *Phys. Rev. D* **98**, 114023 (2018)
- [52] L.-Y. Xiao and X.-H. Zhong, *Phys. Rev. D* **98**, 034004 (2018)
- [53] H.-H. Zhong, R.-H. Ni, M.-Y. Chen, X.-H. Zhong, and J.-J. Xie, *Chin. Phys. C* **47**, 063104 (2023)
- [54] S.-Q. Luo and X. Liu, *Phys. Rev. D* **112**, 014047 (2025)
- [55] T. Gutsche and V. E. Lyubovitskij, *J. Phys. G* **48**, 025001 (2020)
- [56] X. Hu and J. Ping, *Phys. Rev. D* **106**, 054028 (2022)
- [57] Y. Huang, M.-Z. Liu, J.-X. Lu, J.-J. Xie, and L.-S. Geng, *Phys. Rev. D* **98**, 076012 (2018)
- [58] N. Ikeno, W.-H. Liang, G. Toledo, and E. Oset, *Phys. Rev. D* **106**, 034022 (2022)
- [59] N. Ikeno, G. Toledo, and E. Oset, *Phys. Rev. D* **101**, 094016 (2020)
- [60] Y.-H. Lin and B.-S. Zou, *Phys. Rev. D* **98**, 056013 (2018)
- [61] Y. Lin, Y.-H. Lin, F. Wang, B. Zou, and B.-S. Zou, *Phys. Rev. D* **102**, 074025 (2020)
- [62] X. Liu, H. Huang, J. Ping, and D. Chen, *Phys. Rev. C* **103**, 025202 (2021)
- [63] J.-X. Lu, C.-H. Zeng, E. Wang, J.-J. Xie, and L.-S. Geng, *Eur. Phys. J. C* **80**, 361 (2020)
- [64] R. Pavao and E. Oset, *Eur. Phys. J. C* **78**, 857 (2018)
- [65] M. P. Valderrama, *Phys. Rev. D* **98**, 054009 (2018)
- [66] J.-J. Xie and L.-S. Geng, *Chin. Phys. Lett.* **41**, 081402 (2024)
- [67] C.-H. Zeng, J.-X. Lu, E. Wang, J.-J. Xie, and L.-S. Geng, *Phys. Rev. D* **102**, 076009 (2020)
- [68] Q.-H. Shen, J.-X. Lu, L.-S. Geng, X. Liu, and J.-J. Xie (2025)
- [69] Q.-F. Lü, H. Nagahiro, and A. Hosaka, *Phys. Rev. D* **107**, 014025 (2023)
- [70] T. Hyodo and M. Niiyama, *Prog. Part. Nucl. Phys.* **120**, 103868 (2021)
- [71] S. Jia et al., *Phys. Rev. D* **100**, 032006 (2019)
- [72] S. Jia et al., *Phys. Lett. B* **860**, 139224 (2025)
- [73] L. J. Reinders, H. R. Rubinstein, and S. Yazaki, *Phys. Lett. B* **120**, 209 (1983), [Erratum: *Phys.Lett.B* 122, 487 (1983)]
- [74] B. L. Ioffe, *Nucl. Phys. B* **188**, 317 (1981), [Erratum: *Nucl.Phys.B* 191, 591–592 (1981)]
- [75] Y. Chung, H. G. Dosch, M. Kremer, and D. Schall, *Nucl. Phys. B* **197**, 55 (1982)
- [76] D. Jido, N. Kodama, and M. Oka, *Phys. Rev. D* **54**, 4532 (1996)
- [77] J.-P. Zhang, X.-L. Chen, Z.-X. Ou-Yang, X. Yu, W. Chen, and J.-J. Wu, *Phys. Rev. D* **112**, 094047 (2025)
- [78] V. Pascalutsa and D. R. Phillips, *Phys. Rev. C* **67**, 055202 (2003)
- [79] W. Chen, T. G. Steele, H.-X. Chen, and S.-L. Zhu, *Eur. Phys. J. C* **75**, 358 (2015)
- [80] J. M. Dias, F. S. Navarra, M. Nielsen, and C. M. Zanetti, *Phys. Rev. D* **88**, 016004 (2013)
- [81] D.-K. Lian, W. Chen, H.-X. Chen, L.-Y. Dai, and T. G. Steele, *Eur. Phys. J. C* **84**, 1 (2024)
- [82] S. Narison, *Phys. Lett. B* **210**, 238 (1988)
- [83] M. Jamin, J. A. Oller, and A. Pich, *Eur. Phys. J. C* **24**, 237 (2002)
- [84] M. Jamin and A. Pich, *Nucl. Phys. B Proc. Suppl.* **74**,

- 300 (1999)
- [85] H. G. Dosch, M. Jamin, and S. Narison, Phys. Lett. B **220**, 251 (1989)
- [86] A. Khodjamirian, T. Mannel, N. Offen, and Y. M. Wang, Phys. Rev. D **83**, 094031 (2011)
- [87] A. Francis, R. J. Hudspith, R. Lewis, and K. Maltman, Phys. Rev. D **99**, 054505 (2019)
- [88] S. Narison, Nucl. Part. Phys. Proc. **300-302**, 153 (2018)
- [89] Y. Chung, H. G. Dosch, M. Kremer, and D. Schall, Z. Phys. C **25**, 151 (1984)
- [90] S. Narison, Phys. Lett. B **673**, 30 (2009)
- [91] S. Narison, Phys. Lett. B **361**, 121 (1995)
- [92] G.-F. Xu, X.-L. Chen, J.-P. Zhang, N. Li, and W. Chen, Chin. Phys. Lett. **42**, 070201 (2025)
- [93] S.-H. Li, Z.-R. Huang, W. Chen, and H.-Y. Jin (2025)
- [94] S.-H. Li, W.-Y. Lai, and H.-Y. Jin (2025)